ANALYSIS AND DEVELOPMENT OF NEW COMPONENETS FOR A VHCF TEST IN MULTIAXIAL REGIME

Pedro Ferreira Rodrigues da Costa
pedro.r.costa@ist.utl.pt

Instituto Superior Técnico, Universidade de Lisboa, Portugal

January 2017

ABSTRACT

The novel contribution of this paper is the study of very high cycle fatigue done under multiaxial loading, contrary to the standard procedure of uniaxial loading. In ultrasonic fatigue testing, working at 20 kHz, specimens used are hourglass shaped with the purposes of creating a local stress concentration on the expected failure zone. The specimen used under multiaxial loading in ultrasonic fatigue testing has three throats with a circular shape. In order to correctly characterize a material life for this kind of testing, it is necessary to quantify the stress concentration created in the specimen. Thus, the quantification was made through the use of strain gauges applied in the smallest cross-section of each throat. The experimental results are then compared with those obtained by finite element analysis using the ABAQUS commercial software, validating it. With the finite element method created new components were designed, analysed and compared with the initial set. The intensive understanding of the behaviour of the developed test will allow future research on these type of tests, which are pioneer in the world.

KEYWORDS: Ultrasonic fatigue / stress concentration / Multiaxial loading / Very high-cycle fatigue

1. INTRODUCTION

With the use of ultrasonic fatigue testing, it became possible to describe a material behavior, for a uniaxial loading (axial, torsional and bending), for more than 10E7 cycles (VHCF) in a relative short time. The ultrasonic fatigue testing became possible with the use of piezoelectric transducers. Due to the stress concentration and the induced resonance vibration in the specimen, the used equipment requires low loads to achieve high stresses in a high frequency range. [1]

As the understanding of ultrasonic fatigue testing advances, the attention for multiaxial tests becomes the obvious next research step. The complex stresses produced and the high frequency imposed creates the need to fully understand the elastic behavior of the particular geometry of the specimen used under ultrasonic multiaxial fatigue testing.

In order to fully characterize the experimental setup and innovative specimen, it is necessary to research the strains created throughout the ultrasonic test, in particular where the stresses are the most

concentrated, such as the three throats of the used specimen. The comparison of the results of the measured strains in the ultrasonic fatigue test with finite element results will help to understand how close to reality the analytical computational simulation is. This entails a valid method to understand and improve the multiaxial fatigue test under study.

The central throat is the most interesting to research as it is the region where the failure is expected to occur, since it is where the combination of stresses is the highest. The quantification of the concentration stresses on the secondary throats (upper and lower throats) is also important not only to ensure the correct and predicted movement of the specimen during the vibration, but also to ensure the coherence of the analytical results with the experimental results.
Laser experiments were also conducted to understand the movement of the specimen.

2. FATIGUE TESTING MACHINE

The tested experimental set [5] was designed at the mechanical and material test laboratories of DEM, Instituto Superior Técnico, using some of the same machinery developed in [2].

The test aims at imposing multiaxial stresses using an axial transducer. The multiaxial stresses imposed are shear stress through rotation, and normal stress through elongation of the specimen, with the highest stress combination being coincidental on the middle specimen throat. This is only possible due to the particular design created for the horn [5]. This particular horn transforms some of the longitudinal excitation displacement on rotation, having both types of displacement in the base connected to the specimen, and practically no rotation on the opposite base, where it connects to the exciter. A computational representation of the testing device is shown on Fig. 1.

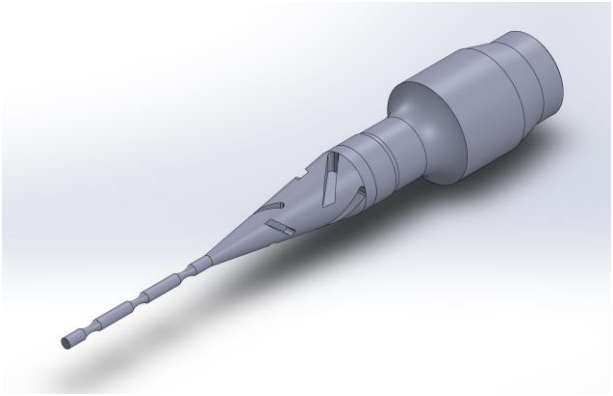

Fig. 1 – Testing device illustration

It is possible to create biaxial stresses in the specimen by exciting it in two simultaneous resonance modes: The first longitudinal mode, Fig. 2, and the third rotational mode, Fig. 3. It can be said that the specimen is in a complex resonance mode.

Fig. 2 –Illustration of the specimens first longitudinal resonance mode

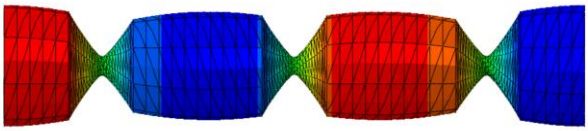

Fig. 3 –Ilustration of the specimens third rotational resonance mode

In Fig. 2. and Fig. 3. it is possible to observe the displacement nodes of each mode in green. These are the places where the stresses should be the highest. In the rotational mode the shear stress should be equal on all three throats. The main throat has a symmetrical shear stress when compared with the secondary ones, for the torsion is opposite.

3. STRAIN MEASUREMENTS

In order to obtain the strain values of interest at all the throats of the specimen, strain gauges were installed, as illustrated in Fig. 4. The three throats of the specimen are the upper throat, closest to the horn, the lower throat, the farthest from the horn, and the central throat. The strain gauges installed are rosette-type strain gauges with the three at 45-degree angles between each other. The strain gauges used are from TML and have the reference FRA-11.

Fig. 4 – Representation of the installed strain gauge

In all experiments, the same components were used (booster, horn, specimen) and the same power was applied, about 1.5% of the transducer capacity. It is also important to acknowledge that the experiment was made using a power control setting. The number of experiments conducted was equal to the total gauge directions in the specimen, three for each rosette-type strain gauge. The data from each strain sensor was obtained separately with the purpose of obtaining the biggest number of points for each cycle. Some preliminary tests were also performed, registering results from pairs of the same rosette-type strain gauge to understand how the three signals were related to each other, namely if they are in phase or in anti-phase strain.

In order to calculate the final stresses, strain values were transformed to the desired axes, and afterwards transformed to stress values using the material properties. The equations method carried out was obtained in [3].

The central throat results were obtained in a previous study [4].

4. LASER MEASUREMENTS

Laser measurements were also carried out with the main purpose of understanding the transverse movement of the specimen. This was achieved by measuring along the specimen’s axis.

Two lasers were used at the same time, one fixed in the upper part of the specimen, and the other moved along the axis for each trial, with the aim of observing the different phases of the movement along the axis and understanding the bending movement detected by the strain gauges.

The results showed that the specimen moved as a pendulum, meaning that the specimen

moved to the same side at the same frequency as the induced vibration. Because it does not have any node along the axis this shows that the bending is not a bending mode of the specimen but a bending mode of the set. A possible description of the displacement of the set's bending is shown in Fig. 5.

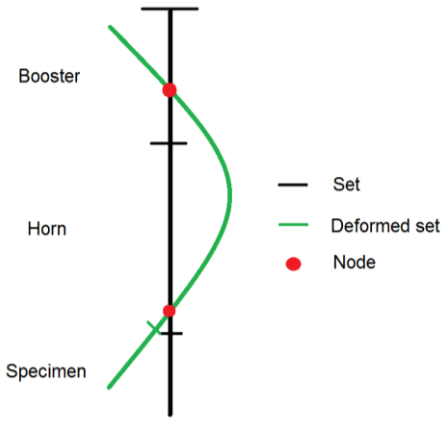

Fig. 5 – Representation of the possible bending in the set

5. FINITE ELEMENT RESULTS

5.1 Finite element method applied

For the finite element analysis of the test set the commercial software Abaqus 6.14-1 was used. All three main components - booster, horn and specimen - were modelled in the analysis, with their respective materials. Elastic, density and Poisson ratio properties were introduced for each material.

In order to obtain stress values for the resonance mode of interest from a dynamic modal analysis, a frequency analysis was initially preformed. Through the frequency analysis of the set components, it is possible to obtain all natural frequencies.

With the known frequency of the resonance mode of interest, a sinusoidal load was created. This load was then applied, in the dynamic modal analysis, at the top of the booster, in the same way the transducer functions in the test. The total force applied will have a sinusoidal variation between the loads of 1N and -1N. The absolute value of the force is not important for this research for two reasons: the method applied on the experiment is through power control, meaning that the extremes of the load may vary along the vibration in order to maintain the resonance of the set; and in the finite element method the extremes of the load are always constant. In this situation only the stress relation between the normal and shear stress is of interest.

In both analyses of finite element, it is required to give the interaction proprieties between all components. A perfect connection was established with no slip and no separation.

For the dynamic modal analysis to have a good resolution of the stress variation in each cycle, the chosen step time was calculated by the following method:

$$St = \frac{1}{f \cdot N} \qquad \textbf{(1)}$$

Where *St* is the step time, *N* the number of calculating points per cycle, and *f* the induced frequency.

If the number of points chosen for each cycle is too low, results will be compromised due to the bad resolution of the force.

5.2 Results

The results show a good correlation between the experimental data.

The shear stress was a little bit higher at the lower throat than to the upper one, as it was obtained by strain measurements. The normal stress is equal for both the upper and the lower throats. An analysis of the normal stress in the throat neighborhood showed that the numerical method does not reproduce the bending obtained in the experiments.

As shown in the Fig. 6 and 7, shear stress and the normal stress are in anti-phase in the secondary throats, and in phase at the main throat. The phases may change depending on the axis used to define them. For any used axis, the phase between axial and shear stresses at the central throat will always be opposite to that at the secondary throats.

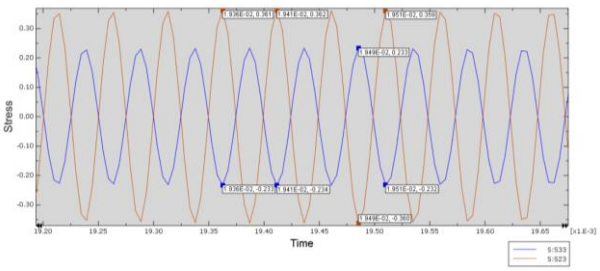

Fig. 6 – Normal (S33) and Shear (S23) stress in the upper throat in the initial set

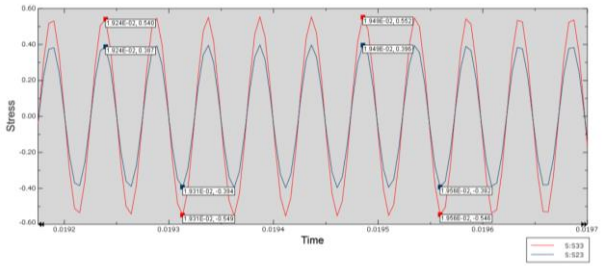

Fig. 7 – Normal (S33) and Shear (S23) stress in the central throat in the initial set

In the point of connection between the horn and the specimen in the initial set, the normal and shear stresses were determined to be roughly 0.38% and 1.18% of the normal and shear stresses at the main throat.

The values do not seem very high, but because they grow with the stresses in the main throat, they could get high enough to break the connection and the resonance of the set.

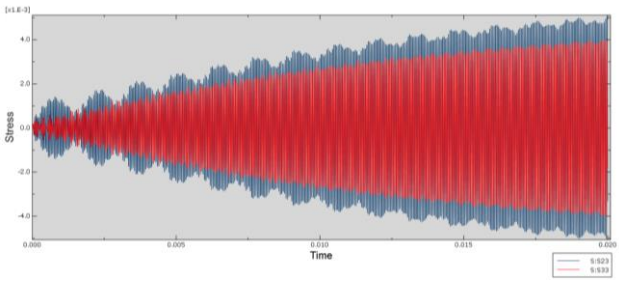

Fig. 8 – Normal (S33) and Shear (S23) stress in the connection point between the horn and the specimen

6. COMPARISON OF RESULTS

The results obtained through the use of strain gauges in the experiment of ultrasonic multiaxial vibration and the results of the finite element in the software Abaqus 6.14-1 are compared for the different stress relations between normal and shear stresses.

Table 1 – Stress relations in all throats and analysis for the initial set

Throats	MatLab (τ /σ)	Abaqus (τ /σ)	Error (%)
Lower	1.142	1.933	69.3
Central	-2/3	-0.718	7.7
Upper	1.457	1.547	6.18

Some deviations are shown between the ratios of the analytical and the experimental stresses, some of which may be related to the quality of information given by the strain gauge or to computational limitations on the developed model. The comparison in the central and upper throat showed best results, where the lower throat has the biggest deviation. The deviation of the results of the lower throat is due to the normal stress being higher than the predicted by the Abaqus commercial program.

The finite element method used did not show any bending movement as the laser and strain gauges proved to be present.

7. PROBLEMS TO BE SOLVED

Through the experimental analysis and the validation of the finite element method applied, it was possible to understand the imperfections of the resonance set under study.

The main problem is the impossibility of applying more than 1.5% of the transducers power.

It was acknowledged that the horn does not have its maximum rotation on the base where it connects with the specimen, creating shear stress in this point. The shear stress will make the connection between the two components slide above 1.5% of the transducer power. A new horn was designed to solve this issue.

The high normal stress detected in the lower throat shows that the specimen has an unwanted bending movement. The laser experiment shows that the movement is not caused by a bending resonance mode of the specimen but of the set. More research is necessary in order to fully understand this situation.

8. NEW COMPONENTS

8.1 New Horn

A new horn was designed with the main purpose of resolving the power issue at hand. After several ideas and trials, it was discovered that the rotation could only be maximum at the smallest radius base by applying a hyperbolic curve to the horn.

An exponential curve was also tested but the results showed that it did not solve the rotation issue.

The final horn has a hyperbolic curve after the second group of rips, as shown in Fig. 9. The figure also shows the maximum rotation on the proper base, and no rotation on the opposite one.

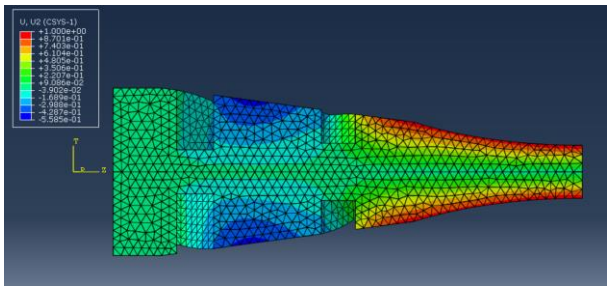

Fig. 9 – Illustration of the rotation on the inside of the hyperbolic horn

The horn was analysed in finite element method through a dynamic modal analysis in conjunction with the booster and the initial specimen. The comparison of the stress relations is showed in table 2.

Table 2 – Stress relations between the initial and new horn

Horn	Throats of the initial specimen		
	Lower (τ /σ)	Central (τ /σ)	Upper (τ /σ)
Initial	1.933	-0.718	1.547
Final	1.257	-0.473	1.039

Table 2 shows that the horn is directly related with the stress relation created.

The new horn was ordered but it did not arrive in time to be tested.

8.2 New specimen

Two different new specimens were designed, both with a higher radius than the existing one. One follows the same geometry than the existing one, and the other has a cone shape between the main throat and secondary throats. Fig. 10 and 11 show an illustration of the two different specimens created.

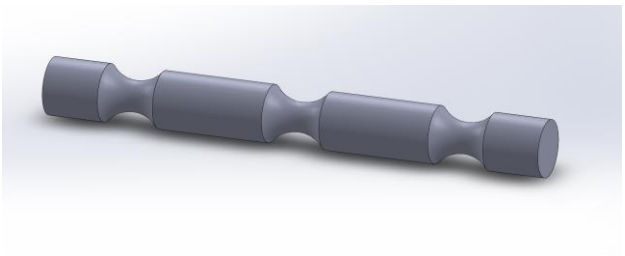

Fig. 10 – Illustration of the new simple specimen

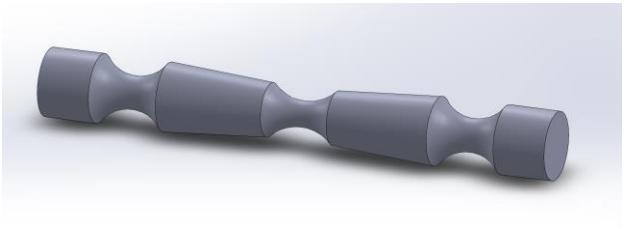

Fig. 11 – Illustration of the new cone shaped specimen

Both specimens were analysed through finite element analysis to see if they improve set deformation, to study stress relation and to compare the normal stress gradient between both geometries and the existing specimen.

The stress relation in each new specimen is shown in table 3. Results show that the specimen geometry is also directly related with the stress relation.

Table 3 – Stress relations for the new specimens with the new horn

Specimen	**Throats**		
	Lower (τ /σ)	**Central** (τ /σ)	**Upper** (τ /σ)
Simple	1.687	-0.728	1.687
Conical	1.909	-0.538	1.909

Stress and displacement nodes show that the resonance mode has a better resolution than the initial set of components.

The stress node at the point of connection between the new horn and the new

specimens is of the most interest, since it is intended to reduce the stress created with a new horn. This node has a smaller and practically negligible value. This proves, at least in the finite element method, that the shear and normal stresses will not affect the connection. And so the set should be able to be excited with higher power from the transducer. The figure shows the shear and normal stress in this node for the cone shaped specimen.

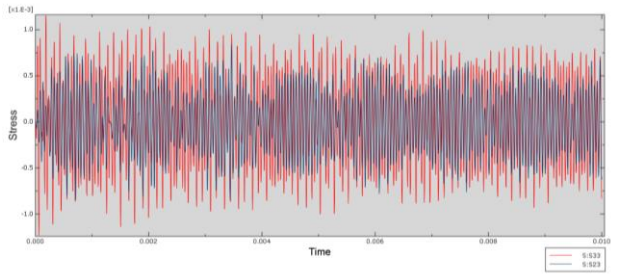

Fig. 12 – Normal (S33) and Shear (S23) stress in the connection point between the new horn and the cone shaped specimen

The shape of the result is completely different from what was obtained with the initial set. The stress values show fluctuations that have a tendency to reduce on average over time. It is assumed that this fluctuation shows that the point where the results are taken is where the node is located. This conclusion follows because on every other point that is not a node, the displacements do not grow with the amplitudes.

For the assumption made, the fluctuations are explained by two sets of reasons.

On the one hand, the frequency at which the load is imposed to the set is never equal to its true natural frequency, because of the existing damping and numerical error. This creates a small movement of the nodes that varies in cycles, as represented in Fig. 12. On the other, these movements are small, more sensitive to numerical error, and so unreasonable spikes are created when displacement is increasing.

Following this assumption, the set with the new horn and specimens shows that some of the nodes are located where they are intended to be, contrary to the results showed by the initial set.

It is also important to remark that the nodes may change their position once the components are attached to each other. This happens because their natural frequencies are not equal. In the case of the initial set, the bad rotation development of the horn forces the rotational nodes of the specimen to be in different places than those predicted. And so only the lower throat showed a rotational node at the small radius cross section.

9. Gradient of the specimens

Is of the interest of the fatigue tests that the normal stress is relatively equal in all the transverse area where the material sample is expected to fail. Due to the concentration stress created in the throats the smallest cross section area of the central throat has a significant gradient.

To study the gradient in the three specimens the mesh was refined in the smallest cross section of the central throat.

Because the new specimens have a bigger radius in the smallest cross section, it was expected a smaller gradient, but it was not found to be the case. Calculating a relation

between the gap of radius and the length of the throats it is observed that the initial specimen has small relation and therefore a smoother gradient. Table 4 shows the relation between the centre and the surface normal stress, following equation (2).

$$\nabla\sigma = \frac{\sigma_{r0}}{\sigma_{\sup}} \quad \textbf{(2)}$$

Table 4 – Stress gradient comparison

Gradient (%)

Initial	Simple	Conical
89	74.8	81.5

The conical shaped specimen makes it easier to obtain a small radius difference in the central throat, in comparison with a simple shaped specimen, thus showing a smaller gradient.

The shear stress has always a gradient because it is proportional to the radius, being zero at the axis. The only way to attenuate it is by using tubular specimens.

10. CONCLUSIONS

Several conclusions follow from the experimental and numerical analyses undertaken in this study.

The strain results showed a higher normal and shear stress in the lower throat when compared with the upper throat. It was predicted that the normal stress was created by a bending mode, and afterwards verified by the laser experiments. The higher shear stress was assumed to be related to the proximity of the node on the smallest cross section of the throat.

Based on the experimental results a valid finite element method was created that enabled to detect and amend the power issue of the initial set. The problem was caused by an incorrect development of the rotation of the horn near the base where it connects to the specimen. The solution was to create a new horn, with higher radius on this base, with the introduction of a hyperbolic curve. The higher radius also allows a higher surface connection to secure the slip between the specimen and the horn.

New specimens with higher radiuses were modelled to compare the new set with the initial one, and to understand how the normal stress gradient can be reduced in the smallest cross section of the specimen.
Because the specimen geometry influences the stress relation obtained, as it was verified, the final specimen selected for testing has to be designed taking into account the intended stress relation. It is of interest to create a model that relates the stress relation and the geometry of the specimen for a specific horn.

The results of the new set showed that the new surpasses the initial one. Its resonance mode showed a better development of the displacements in the specimen. Not only the stress created in the connection point between the horn and the specimen has lower

values, but it also shows that the tension node should be in this point. The new set also has a smaller difference in shear stress between the secondary throats.

The experiments conducted do not fully explain the bending mode detected. They only showed that it is not a resonance mode of the specimen, but of the set itself. The bending was not replicated in the finite element method. A more thorough investigation is needed in order to fully understand how and why the bending mode occurs.

REFERENCES

[1] Bathias, C., & Paris, P. C. (2005). *Gigacycle Fatigue in Mechanical Practice (1º ed.)*. New York: Marcel Dekker.

[2] Freitas, M., Reis, L., Anes, V., Montalvão, D., Ribeiro, A. M. & Fonte, M. (2011). "Design and Assembly of na Ultrasonic Fatigue Testing Machine", *Anales de Mecánica de la Fractura*, Vol. 1: 335-340.

[3] Milner, P., (1989). "A modern approach to principal stresses and strains", *School of Science and Technology*, Volume 25, Issue 4.

[4] Vieira, M., Reis, L., Freitas, M., & Ribeiro, A. (2016). "Strain Measurements on specimens subjected to biaxial ultrasonic fatigue testing". *Theoretical and Applied Fracture Mechanics*.

[5] Vieira, M., Freitas, M. d., Reis, L., Ribeiro, A. M., & Fonte, M. d. (2016). "Development of a very high cycle fatigue (VHCF) multiaxial testeing device". *International Conference on Multiaxial Fatigue & Fracture*, 37, 131-137.